REGULAR PAPER

Eszter Farkas · Gergely Donka · Rob A. I. de Vos
András Mihály · Ferenc Bari · Paul G. M. Luiten

Experimental cerebral hypoperfusion induces white matter injury and microglial activation in the rat brain

Abstract Though cerebral white matter injury is a frequently described phenomenon in aging and dementia, the cause of white matter lesions has not been conclusively determined. Since the lesions are often associated with cerebrovascular risk factors, ischemia emerges as a potential condition for the development of white matter injury. In the present study, we induced experimental cerebral hypoperfusion by permanent, bilateral occlusion of the common carotid arteries of rats ($n=6$). A sham-operated group served as control ($n=6$). Thirteen weeks after the onset of occlusion, markers for astrocytes, microglia, and myelin were found to be labeled by means of immunocytochemistry in the corpus callosum, the internal capsule, and the optic tract. The ultrastructural integrity and oligodendrocyte density in the optic tract were investigated by electron microscopy. Quantitative analysis revealed that chronic cerebral hypoperfusion caused mild astrogliosis in the corpus callosum and the internal capsule, while astrocytic disintegration in the optic tract increased by 50%. Further, a ten-fold increase in microglial activation and a nearly doubled oligodendrocyte density were measured in the optic tract of the hypoperfused rats as compared with the controls. Finally, vacuolization and irregular myelin sheaths were observed at the ultrastructural level in the optic tract. In summary, the rat optic tract appears to be particularly vulnerable to ischemia, probably because of the rat brain's angioarchitecture. Since the detected glial changes correspond with those reported in vascular and Alzheimer dementia, this model of cerebral hypoperfusion may serve to characterize the causal relationship between ischemia and white matter damage.

Keywords Astrocyte · Cerebral hypoperfusion · Microglia · Optic tract · White matter

Introduction

Magnetic resonance imaging (MRI) and computed tomography (CT) scans have frequently detected subcortical and periventricular white matter lesions as hyperintensive territories in elderly and demented patients [1, 2, 3, 11, 15]. By means of basic histological staining techniques in post-mortem tissue, such white matter injury has been identified as myelin rarefaction, while specific markers have indicated demyelination [31], the loss of fine myelinated fibers [30], the apoptosis of oligodendrocytes [16, 20], gliosis [25], and regressive astrocytic changes [32].

Although the exact cause of this white matter pathology has not been conclusively established, white matter lesions have frequently been suggested to have a vascular origin. For example, chronic cerebral hypoperfusion and focal ischemia have been proposed as vascular risk factors for white matter injury [14, 15]. In order to test this hypothesis, experimental cerebral hypoperfusion was created in rats by permanent, bilateral occlusion of the common carotid arteries [two-vessel occlusion (2VO)]. The occlusion caused an initial 60–70% drop in the regional cerebral blood flow in the corpus callosum, which stabilized at a value of 52–64% of the original flow at 30 days after the ligation [33]. The consequent white matter damage was investigated by histological techniques at various time points after the ligation. Axonal damage and demyelination were indicated, for instance, by an increased amyloid precursor protein expression and encephalitogenic peptide signals up to 30 days after the onset of 2VO [35]. Oligodendrocyte degeneration appeared in the form

E. Farkas (✉) · G. Donka · A. Mihály
Department of Anatomy, School of Medicine,
University of Szeged, PO Box 427, 6701 Szeged, Hungary
Tel.: +36-62-545669, Fax: +36-62-545707,
e-mail: farkase@anat-fm.szote.u-szeged.hu

E. Farkas · P. G. M. Luiten
Department of Molecular Neurobiology,
University of Groningen, Groningen, The Netherlands

R. A. I. de Vos
Laboratory for Pathology, Enschede, The Netherlands

F. Bari
Department of Physiology, School of Medicine,
University of Szeged, Szeged, Hungary

of apoptotic cell death, which was visualized with the TUNEL method and caspase-3 RNA detection [33]. Moreover, an elevated matrix metalloprotease-2 (MMP-2) or major histocompatibility complex class I and II (MHC-I/II) expression at 3 days hypoperfusion demonstrated microglial activation [13, 34], pointing to an early neuroinflammatory reaction after the onset of cerebral hypoperfusion. Additionally, the histological abnormalities were associated with a compromised function. For instance, damage to the optic tract following 2VO in rats was related to the loss of pupillary reflex from 5 days after surgery [6].

The above findings collectively address different aspects of ischemia-related white matter damage; nevertheless, it remains to be elucidated how the astrocytic, microglial, and oligodendrocytic changes are spatially and temporally related.

In the present study, we set out to identify cerebral hypoperfusion-induced white matter changes in rats that may correspond with features of human white matter lesions. We made use of the 2VO rat model to characterize interrelated astroglial, microglial, and oligodendroglial changes that can evolve as a result of a chronically reduced cerebral blood flow. Since the regional distribution of the white matter in the rat brain differs from that in the human brain (e.g., an equivalent of the human centrum semiovale cannot be outlined in the rat brain), the corpus callosum, internal capsule, and optic tract were chosen as regions of interest. The results are discussed in the light of previous human and experimental findings on cerebral white matter injury.

Materials and Methods

Surgery

The animal experiments were conducted in accordance with prevailing laws on animal experiments and were approved by the ethical committee of the University of Szeged. Twelve male Wistar rats (210±10 g) were anesthetized with 400 mg/kg chloral hydrate i.p. followed by 0.05 ml atropine i.m. The common carotid arteries were exposed via a ventral cervical incision and separated from their sheaths and vagal nerves. Experimental cerebral hypoperfusion was induced by permanent 2VO in half of the animals, while the other half served as sham-operated controls (SHAM) [9]. The same surgical procedure was performed in the SHAM group but without the actual ligation.

Thirteen weeks later, the animals were anesthetized with an overdose of pentobarbital and perfused transcardially with 100 ml saline followed by 400 ml 3.5% paraformaldehyde and 0.5% picric acid in 0.1 M phosphate buffer (PB, pH=7.4). The brains were removed, one hemisphere was postfixed in the same solution for up to 1 h and then stored in 0.1 M PB for immunocytochemical investigations. The other hemisphere was postfixed and stored in 2.5% glutaraldehyde and 2% paraformaldehyde in 0.1 M PB.

Immunocytochemistry

Free-floating coronal sections of one hemisphere were cut at 20 μm thickness on a cryostat microtome and collected in 0.1 M PB. Slices at Bregma –3.14 mm [22] were immunocytochemically stained for glial fibrillary acidic protein (GFAP) to visualize astrocytic proliferation. Briefly, sections were treated with 0.3% H_2O_2 in phosphate-buffered saline (PBS) and preincubated in 5% normal

sheep serum (NShS). The samples were then incubated in a primary antibody solution containing mouse anti-GFAP antibody (Sigma), 1:200, 1% NShS, and 0.3% Triton X-100 in 0.01 M PBS, overnight at 37°C. The secondary antibody solution consisted of sheep anti-mouse biotinylated IgG (Jackson), 1:200, and 0.3% Triton X-100 in 0.01 M PBS for 2 h at room temperature (RT). Finally, the sections were incubated in HRP-Streptavidine (Zymed), 1:200, for 2 h at RT, and the color reaction was conventionally developed with diaminobenzidine (DAB) and H_2O_2.

To detect and analyze microglial activation over the white matter areas, the cell-surface marker OX-42 was used on a second set of sections. The procedure started with washing and pretreatment of the samples with 0.5% Triton X-100 and 3% H_2O_2 in 0.01 M PBS followed by preincubation in 20% normal porcine serum (NPS) and 0.5% Triton X-100 in 0.01 M PBS for 1 h. The sections were incubated in a primary antibody solution containing biotinylated mouse anti-CD11b antibody (OX-42, Serotec), 1:500, 20% NPS, and 0.03% merthiolate in 0.01 M PBS overnight at RT. Next, the sections were rinsed and then incubated in a solution of STA-PER (Jackson), 1% NPS, and 0.03% merthiolate in 0.1 M Tris buffer for 1 h at RT. Finally, the color reaction was developed by nickel-DAB and H_2O_2.

Myelin basic protein (MBP) immunocytochemistry was performed as follows: Sections were treated with a solution of 0.5% Triton X-100 and 3% H_2O_2 in 0 01 M PBS followed by preincubation in 20% NPS. The samples were then kept in a primary antibody solution containing mouse anti-MBP antibody (Chemicon), 1:100, 20% NPS, and 0.03% merthiolate in 0.01 M PBS overnight at RT. After washing steps in PBS, the sections were incubated in a secondary antibody solution of biotinylated goat anti-mouse IgG (Jackson), 1:400, 10% NPS, and 0.03% merthiolate in 0.01% Tris buffer for 1 h at RT followed by a solution of STA-PER (Jackson), 1% NPS, and 0.03% merthiolate in 0.1 M Tris buffer for 1 h at RT. Finally, the color reaction was developed with nickel-DAB and H_2O_2. All the sections were mounted on gelatin-coated microscopic slides, air-dried, dehydrated, and coverslipped with DPX.

The percentage surface area of GFAP-positive astrocytes in the medial corpus callosum and the internal capsule was quantified by using a Quantimet Q-600HR computerized image analysis system (Leica, Cambridge, UK) with a 469.4-nm emission filter [12]. Briefly, three consecutive coronal sections with a standard distance of 160 μm, starting at Bregma –3.14 mm [22], were selected for the analysis. Regions of interest were manually delineated at 10× magnification after background subtraction and gray scale threshold determination. The area covered by GFAP-positive astrocytes was computed as a percentage of the total area delineated. The measured results on the three sections per animal were averaged, and this average value was used for further statistical analysis. For the optic tract, relative optical density was computed instead of area percentage, since the homogenous labeling did not permit area measurements.

The section area covered by OX-42 immunoreactive microglia was quantified in a similar manner as for GFAP-labeled sections on a computerized image analysis system (Olympus BX50, DP50, software: ImagePro Plus, Media Cybernetics). The degree of MBP immunoreactivity was determined by measuring the optical densities of delineated regions following the above guidelines (Olympus BX50, DP50, software: ImagePro Plus).

Finally, the thickness of the corpus callosum, the internal capsule, and the optic tract was measured and expressed in micrometers in the MBP-stained sections by using the same software (ImagePro Plus). The thickness of the individual regions was determined in three consecutive sections per animal. The averages of the three measurements per rat were used for further statistical analysis. Data were analyzed statistically by one-way ANOVA testing with the software SPSS.

Electron microscopy

Based on the data obtained by immunocytochemistry, optic tract samples of the other hemisphere were processed for electron microscopy [10]. Briefly, after thorough rinsing, tissue blocks were
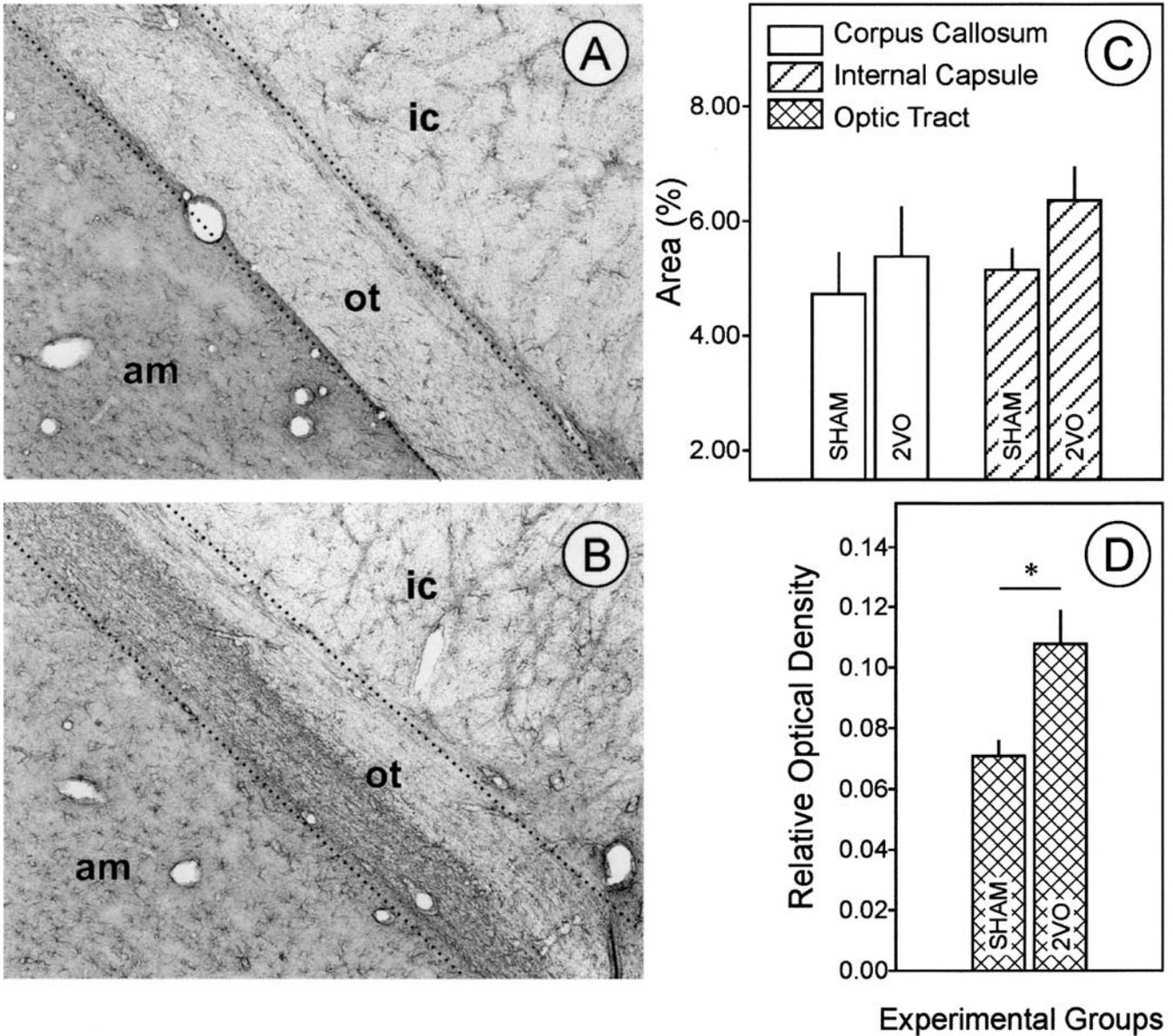
Fig. 1A–D Photomicrographs and quantitative data on glial fibrillary acidic protein (GFAP)-positive astrocytic proliferation. **A** Optic tract of a sham-operated controls (SHAM) animal. **B** Optic tract of a bilateral carotid artery occlusion (2VO) animal. Pictures were taken at 10× magnification. **C, D** Quantitative data on astrocytic proliferation in the corpus callosum, the internal capsule, and the optic tract, $p* < 0.05$. *am* amygdala complex, *ic* internal capsule, *ot* optic tract

A tissue surface area of $800 \mu m^2$ (~10 grid holes) was scanned. The exact surface area in each case was defined on the basis of the number of investigated grid holes of standard size. The number of oligodendrocyte nuclei on the given surface was counted, and oligodendrocyte density per $10 \mu m^2$ was calculated. Results were analyzed statistically with a one-way ANOVA model via the software SPSS.

incubated in an aqueous solution of 1% OsO_4 and 5% $K_2Cr_4O_7$ (1:1). Subsequently, the samples were dehydrated, incubated in 1% uranyl acetate, and embedded in Durcupan epoxy resin (Fluka). Semithin sections were cut on an ultramicrotome (Ultracut E, Reichert-Jung) and stained on object glasses with a 1:1 mixture of 1% methylene blue and 1% azure II blue. The samples were next coverslipped with DPX and analyzed under a light microscope (Nikon E600). Ultrathin sections were cut from the same blocks and collected on 200-mesh copper grids. The preparations were then contrasted with 5% uranyl acetate and Reynolds lead citrate solution. Finally, the samples were analyzed with a Philips TM10 transmission electron microscope. Photographs were taken with a computer-assisted digital camera.

Results

Hypoperfusion-induced white matter injury in the rat brain was characterized in the corpus callosum, the internal capsule, and the optic tract. GFAP-positive astrocytes were distributed sparsely in the white matter regions in the SHAM animals (Fig. 1A), whereas a dense immunolabeling was observed in the 2VO rats, particularly in the optic tract. In the corpus callosum and the internal capsule, astrocytic perikarya and processes were well discernible, while the homogeneous GFAP immunoreactivity in the
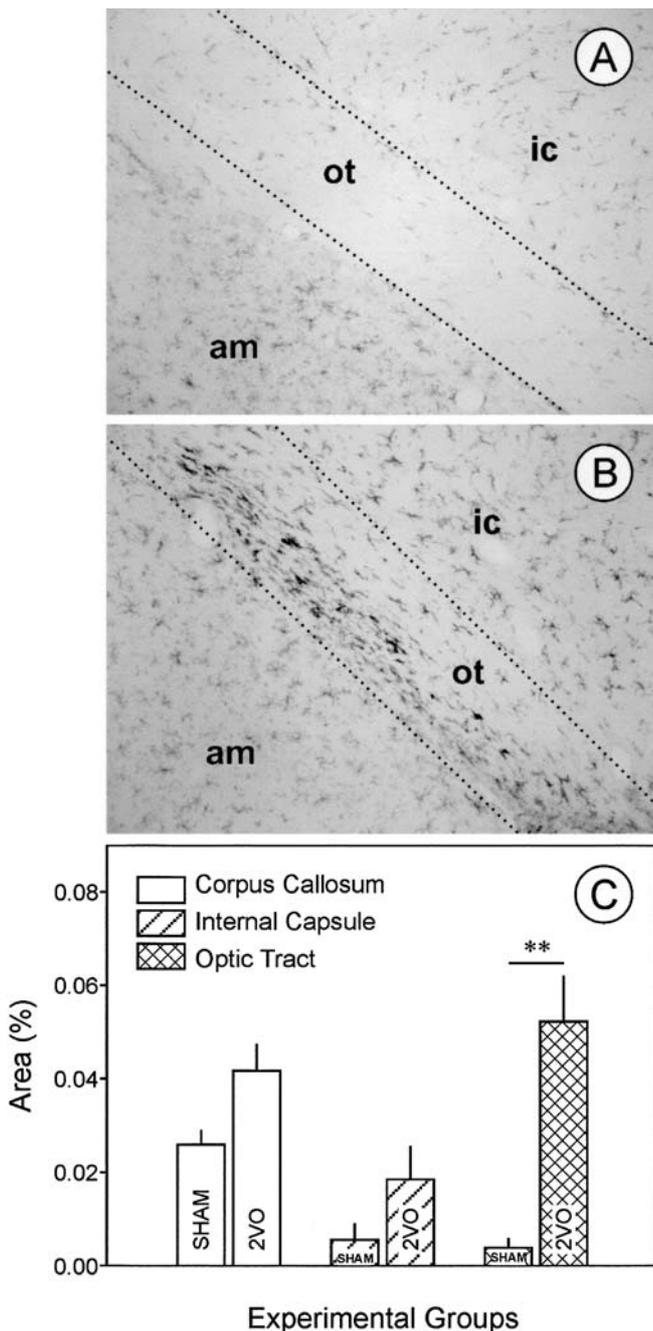
Fig. 2A–C Photomicrographs and quantitative data on OX-42-positive microglial activation. **A** Optic tract of a sham-operated control (SHAM) animal. **B** Optic tract of a bilateral carotid artery occlusion (2VO) animal. Pictures were taken at 10× magnification. **C** Quantitative data on microglial activation in the corpus callosum, the internal capsule, and the optic tract, $p** < 0.01$. *am* amygdala complex, *ic* internal capsule, *ot* optic tract

optic tract appeared to denote astrocytic disintegration (Fig. 1B). Quantitative analysis revealed that the area covered by astrocytes in the 2VO rats was moderately increased in the corpus callosum and the internal capsule (Fig. 1C). At the same time, GFAP immunoreactivity was significantly denser in the optic tract of the 2VO rats as compared with the SHAM controls (Fig. 1D).

The microglial activation visualized by OX-42 labeling displayed a similar pattern. The white matter regions in the SHAM animals were either devoid of immunoreactive microglia or contained a very few labeled cells (Fig. 2A). On the other hand, a marked microglial activity was detected in the 2VO rats, particularly in the optic tract (Fig. 2B). Furthermore, the affected area coincided with that densely labeled for GFAP. Quantitative analysis demonstrated increased microglial activation in all three investigated white matter regions, most strikingly in the optic tract (Fig. 2C). More specifically, the proportion of the microglia-covered area was doubled in the corpus callosum and the internal capsule and increased more than ten-fold in the optic tract of the 2VO rats as compared with the controls.

Myelin density was determined by means of MBP immunocytochemistry, which at high contrast delineated white matter in both groups (Fig. 3A and B). Mild increases in MBP density were detected in the regions of interest in the 2VO rats. Particularly the optic tract demonstrated an elevated optical density, which corresponded in localization with the increased GFAP and OX-42 signals (Fig. 3B). However, the group differences were not significant statistically (Fig. 3C). On the other hand, oligodendrocyte density exhibited a 1.6-fold increase, as determined by electron microscopy (Fig. 3D).

The thickness of the internal capsule was found to be similar in the two experimental groups. The corpus callosum and the optic tract appeared narrower in the 2VO animals than in the SHAM group. The average thickness of the corpus callosum in the SHAM animals was 376 μm, whereas in the 2VO group, it was only 211 μm. In the optic tract, the thickness of the structure in the SHAM group was 328 μm, while in the 2VO group, it was 283 μm. However, the changes were not significant statistically.

The ultrastructural investigation of the optic tract revealed marked degenerative changes. Large vacuoles among the axons filled with homogenous material were observed in all the 2VO animals (Fig. 4A and B). The myelin sheath layers embracing the axons were loose and irregular, often penetrating into the axonal cross-section (Fig. 4C and D). Different stages of axonal degeneration could be seen in the form of swollen cross-sections surrounded by a disintegrating myelin sheath, or electron-dense deposits with complete myelin degeneration. Moreover, the microglia could be clearly distinguished, often tightly apposed to abnormal fibers. Regressive changes in the astrocyte processes were detected in the form of extensive swelling and a lack of intracellular compartments. Very few blood vessels were encountered in which the walls seemed to be normal. No basement membrane pathology or irregular pinocytic transport was observed.

Discussion

In the present study, we encountered glial changes in chronic cerebral hypoperfusion-induced white matter damage. Thirteen weeks after the onset of hypoperfusion, we detected region-specific mild astrogliosis in the corpus cal-
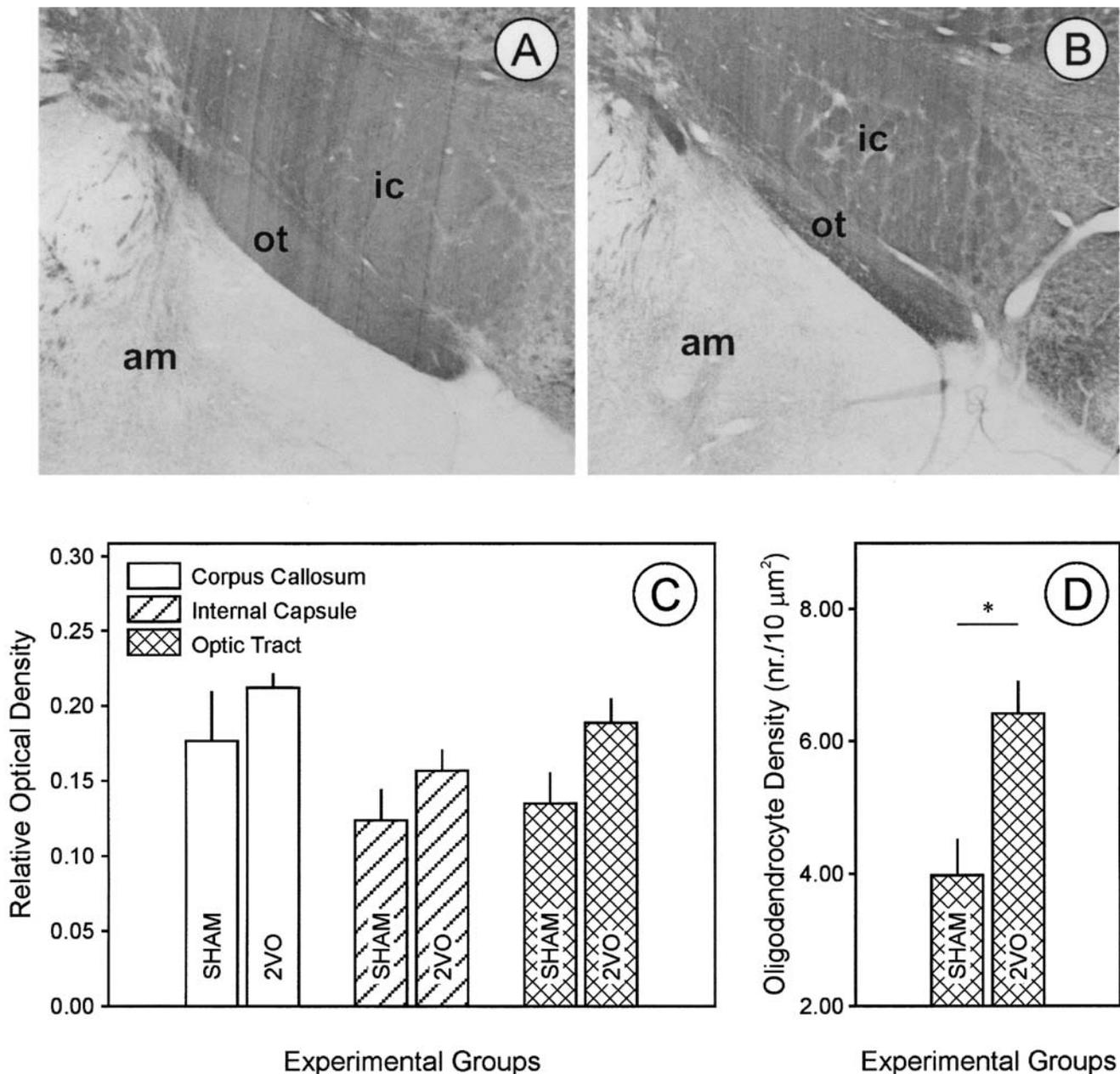
Fig. 3A–D Photomicrographs and quantitative data on myelin-basic-protein (MBP)-positive myelin density. **A** Optic tract of a sham-operated control (SHAM) animal. **B** Optic tract of a bilateral carotid artery occlusion (2VO) animal. Pictures were taken at 4× magnification. **C** Quantitative data on MBP density in the corpus callosum, the internal capsule, and the optic tract. **D** Quantitative data on oligodendrocyte density in the optic tract, $p* < 0.05$. *am* amygdala complex, *ic* internal capsule, *ot* optic tract

losum and the internal capsule, or astrocytic disintegration in the optic tract, marked microglial activation, an increased oligodendrocyte density, and myelin damage.

As a typical degenerative feature, we observed extensive vacuolization, particularly in the optic tract, which accords with previous reports [29]. Such vacuoles may contribute to the lesions generally referred to as white matter rarefaction [8, 21].

The optic tract was the preferential site of white matter damage, the astrocytes and microglia being most severely affected here. The accentuated vulnerability of the optic tract in ischemia-related white matter injury has also been observed by others [29, 35]. Such region specificity could very well originate in the vascular architecture of the rat brain. The optic nerves and tracts are supplied by direct branches of the internal carotid arteries, while the corpus callosum receives arterial blood from the uniting anterior cerebral arteries, and the internal capsule does so from the middle cerebral artery [26, 36]. Since the compensatory redistribution in the circle of Willis after carotid-artery occlusion is not immediate and definitely not absolute, selected brain regions such as the optic tract may suffer more severe ischemic damage.

All three types of immunocytochemical staining here showed that the lateral part of the optic tract displayed the
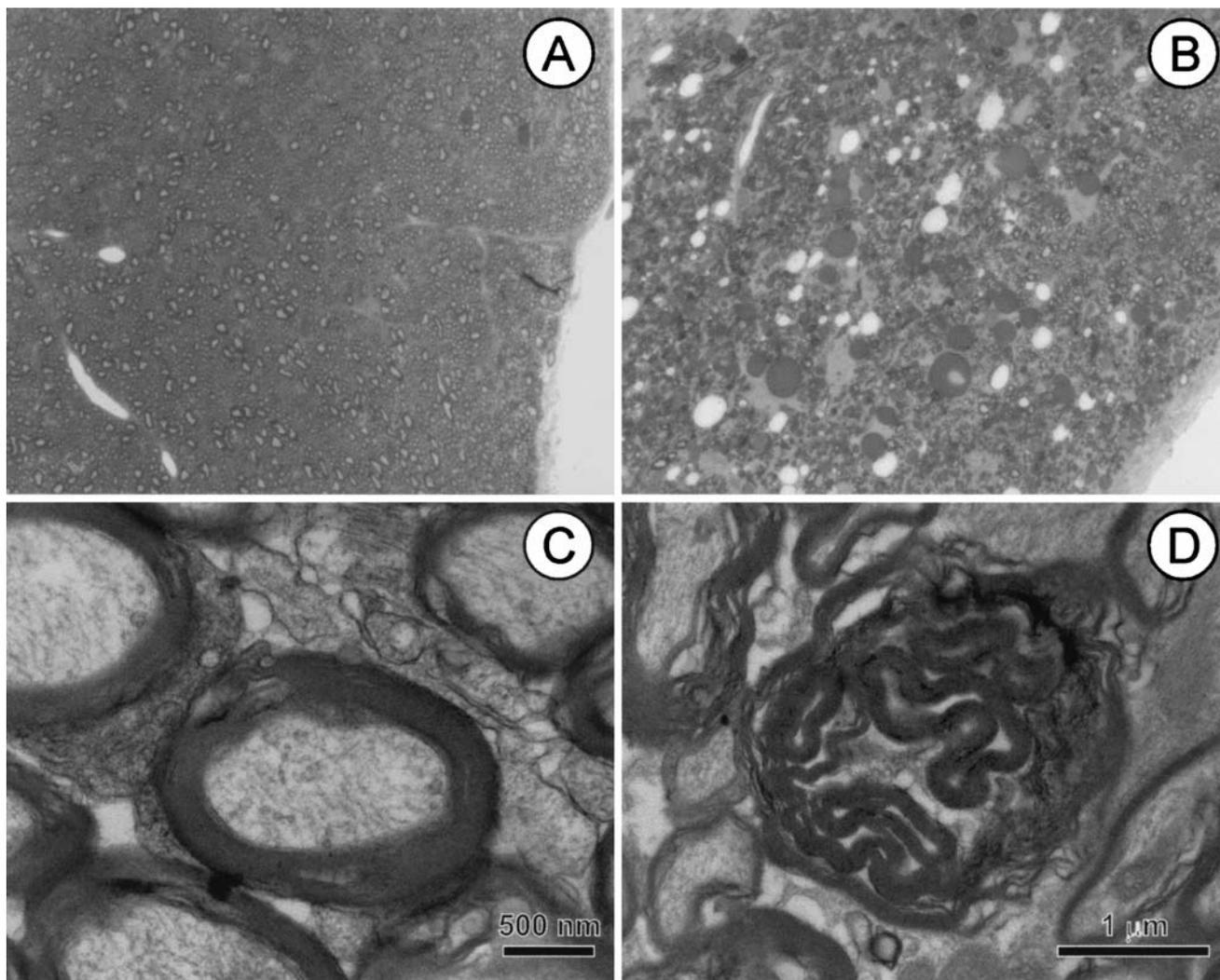
Fig. 4A–D Semithin and ultrathin images of white matter degeneration. **A** Semithin section of the optic tract, sham-operated control (SHAM) animal, original magnification: 40×. **B** Semithin section showing vacuolization in the optic tract, bilateral carotid artery occlusion (2VO) animal, original magnification: 40×. **C** Electron microscopic image of an intact myelinated axon, SHAM animal. **D** Electron microscopic image of a degenerating myelinated axon, 2VO animal

most striking degenerative changes, while the medial portion remained relatively intact. The reason for this selective vulnerability is unclear. The topographical organization of the fibers (segregation according to retinotopic origin) [4, 5] may play a role in a selective susceptibility to ischemia. Alternatively, the medial optic tract may benefit from its close proximity to the internal capsule, which is supplied by the middle cerebral artery [26]. Branches of the middle cerebral artery reaching the medial optic tract may render the region more resistant to hypoperfusion.

The astrocytic changes found here can be divided into two categories: mild gliosis in the corpus callosum and the internal capsule, and pronounced regressive changes in the optic tract. Astrocytes can react to ischemia in different ways depending on the length and severity of the insult. In the early ischemic period, the astrocytes respond with proliferation, while the persistence of hypoperfusion causes progressive astrocytic degeneration and eventually cell death [28, 33, 37]. Given that the length of hypoperfusion was standard for the entire brain in our model, the varying severity of ischemia may be responsible for the area-dependent astrocytic reactivity. Interestingly, in the white matter and the frontal cortex of demented patients, GFAP-labeled astrocytes also exhibited disintegration and regression, which was associated with ischemia [19, 32]. The present experimental data strongly support the concept that hypoperfusion-induced astrocytic damage can contribute to the white matter lesions that occur in aging and dementia.

We have found extensive OX-42-positive microglial activation in the white matter areas and particularly in the optic tract. Our data demonstrate that microglial activation is long lasting: up to 13 weeks after the onset of chronic cerebral hypoperfusion. These results complement previous observations, which demonstrated that activated microglia-expressed MMP-2 or MHC-I/II in the rat optic tract and the corpus callosum shortly after the onset of ischemia [13, 34]. Microglial activation in the white matter of dementia patients has been detected with several

markers. Microglia obtained from the white matter on the autopsy of vascular or Alzheimer dementia patients were immunoreactive to MHC-II, MMP-3, and proinflammatory cytokines [7, 18, 24]. Since microglia can promote delayed neuronal damage by generating proinflammatory cytokines or may participate in regenerative processes by scavenging necrotic tissue [17, 27], microglial activation in cerebral hypoperfusion can be a sign of such processes in the white matter.

Finally, we detected an increased MBP and oligodendrocyte density in the optic tract of the 2VO rats. Since other reports on white matter lesions often describe a myelin loss [30, 35], our finding may appear controversial. We observed structural abnormalities of the myelin sheaths, but this does not directly indicate the loss of myelin. The view that myelin degeneration is accompanied by the formation of redundant myelin and an increased number of oligodendrocytes in aging [23] can be regarded as supporting evidence. However, we believe that the increased MBP signal and the corresponding rise in oligodendrocyte density in our material may arise from tissue shrinkage, since these factors coincided with a decreased thickness of the regions.

In summary, the present study involved a comprehensive analysis of white matter changes in the rat brain after chronic cerebral hypoperfusion. The results indicate that white matter degeneration is region specific and is probably related to the severity of ischemia in the particular regions. In this respect, the 2VO model of chronic cerebral hypoperfusion emerges as a model for the characterization of cellular changes in human white matter injury, even if there is not a strict regional correspondence between rat and human.

References

1. Barber R, Gholkar A, Scheltens P, Ballard C, McKeith IG, O'Brien JT (2000) MRI volumetric correlates of white matter lesions in dementia with Lewy bodies and Alzheimer's disease. Int J Geriatr Psychiatry 15(10):911–916
2. Barkhof F, Scheltens P (2002) Imaging of white matter lesions. Cerebrovasc Dis 13 [Suppl 2]:21–30
3. Bartzokis G, Cummings JL, Sultzer D, Henderson VW, Nuechterlein KH, Mintz J (2003) White matter structural integrity in healthy aging adults and patients with Alzheimer disease: a magnetic resonance imaging study. Arch Neurol 60(3): 393–398
4. Chan SO, Guillery RW (1994) Changes in fiber order in the optic nerve and tract of rat embryos. J Comp Neurol 344(1): 20–32
5. Chelvanayagam DK, Dunlop SA, Beazley LD (1998) Axon order in the visual pathway of the quokka wallaby J Comp Neurol 390(3):333–341
6. Davidson CM, Pappas BA, Stevens WD, Fortin T, Bennett SA (2000) Chronic cerebral hypoperfusion: loss of pupillary reflex, visual impairment and retinal neurodegeneration. Brain Res 859(1):96–103
7. de Groot CJ, Hulshof S, Hoozemans JJ, Veerhuis R (2001) Establishment of microglial cell cultures derived from post-mortem human adult brain tissue: immunophenotypical and functional characterization. Microsc Res Tech 54(1):34–39
8. Englund E (1998) Neuropathology of white matter changes in Alzheimer's disease and vascular dementia. Dement Geriatr Cogn Disord 9 [Suppl 1]:6–12
9. Farkas E, de Wilde MC, Kiliaan AJ, Meijer J, Keijser JN, Luiten PG (2002) Dietary long chain PUFAs differentially affect hippocampal muscarinic 1 and serotonergic 1A receptors in experimental cerebral hypoperfusion. Brain Res 954(1): 32–41
10. Farkas IG, Czigner A, Farkas E, Dobo E, Soos K, Penke B, Endresz V, Mihaly A (2003) Beta-amyloid peptide-induced blood-brain barrier disruption facilitates T-cell entry into the rat brain. Acta Histochem 105(2):115–125
11. Fazekas F, Schmidt R, Kleinert R, Kapeller P, Roob G, Flooh E (1998) The spectrum of age-associated brain abnormalities: their measurement and histopathological correlates. J Neural Transm [Suppl 53]:31–39
12. Horvath KM, Abraham IM, Harkany T, Meerlo P, Bohus BG, Nyakas C, Luiten PGM (2000) Postnatal treatment with ACTH-(4–9) analog ORG 2766 attenuates N-methyl-D-aspartate-induced excitotoxicity in rat nucleus basalis in adulthood. Eur J Pharmacol 405(1–3):33–42
13. Ihara M, Tomimoto H, Kinoshita M, Oh J, Noda M, Wakita H, Akiguchi I, Shibasaki H (2001) Chronic cerebral hypoperfusion induces MMP-2 but not MMP-9 expression in the microglia and vascular endothelium of white matter. J Cereb Blood Flow Metab 21(7):828–834
14. Irving EA, Bentley DL, Parsons AA (2001) Assessment of white matter injury following prolonged focal cerebral ischaemia in the rat. Acta Neuropathol (Berl) 102(6):627–635
15. Kobari M, Meyer JS, Ichijo M, Oravez WT (1990) Leukoaraiosis: correlation of MR and CT findings with blood flow, atrophy, and cognition. Am J Neuroradiol 11(2):273–281
16. Kobayashi K, Hayashi M, Nakano H, Fukutani Y, Sasaki K, Shimazaki M, Koshino Y (2002) Apoptosis of astrocytes with enhanced lysosomal activity and oligodendrocytes in white matter lesions in Alzheimer's disease. Neuropathol Appl Neurobiol 28(3):238–251
17. Lees GJ (1993) The possible contribution of microglia and macrophages to delayed neuronal death after ischemia. J Neurol Sci 114(2):119–122
18. Lue LF, Rydel R, Brigham EF, Yang LB, Hampel H, Murphy GM Jr, Brachova L, Yan SD, Walker DG, Shen Y, Rogers J (2001) Inflammatory repertoire of Alzheimer's disease and nondemented elderly microglia in vitro. Glia 35(1):72–79
19. Martin JA, Craft DK, Su JH, Kim RC, Cotman CW (2001) Astrocytes degenerate in frontotemporal dementia: possible relation to hypoperfusion. Neurobiol Aging 22(2):195–207
20. Masumura M, Hata R, Nagai Y, Sawada T (2001) Oligodendroglial cell death with DNA fragmentation in the white matter under chronic cerebral hypoperfusion: comparison between normotensive and spontaneously hypertensive rats. Neurosci Res 39(4):401–412
21. Nanri M, Miyake H, Murakami Y, Matsumoto K, Watanabe H (1998) Chronic cerebral hypoperfusion-induced neuropathological changes in rats. Nihon Shinkei Seishin Yakurigaku Zasshi 18(5):181–188
22. Paxinos G, Watson C. (1986) The rat brain in stereotactic coordinates, 2nd edn, Academic Press, New York
23. Peters A (2002) The effects of normal aging on myelin and nerve fibers: a review. J Neurocytol 31(8–9):581–593
24. Rosenberg GA, Sullivan N, Esiri MM (2001) White matter damage is associated with matrix metalloproteinases in vascular dementia. Stroke 32(5):1162–1168
25. Scheltens P, Barkhof F, Leys D, Wolters EC, Ravid R, Kamphorst W (1995) Histopathologic correlates of white matter changes on MRI in Alzheimer's disease and normal aging. Neurology 45(5):883–888

26. Scremin OU (1995) Cerebral Vascular System. In: Paxinos G, ed, The rat nervous system, 2nd edn, Academic Press, New York, pp 3–35

27. Stoll G, Jander S, Schroeter M (1998) Inflammation and glial responses in ischemic brain lesions. Prog Neurobiol 56(2): 149–171

28. Sugawara T, Lewen A, Noshita N, Gasche Y, Chan PH (2002) Effects of global ischemia duration on neuronal, astroglial, oligodendroglial, and microglial reactions in the vulnerable hippocampal CA1 subregion in rats. J Neurotrauma 19(1):85–98

29. Takizawa S, Fukuyama N, Hirabayashi H, Kohara S, Kazahari S, Shinohara Y, Nakazawa H (2003) Quercetin, a natural flavonoid, attenuates vacuolar formation in the optic tract in rat chronic cerebral hypoperfusion model. Brain Res 980(1):156–160

30. Tang Y, Nyengaard JR, Pakkenberg B, Gundersen HJ (1997) Age-induced white matter changes in the human brain: a stereological investigation. Neurobiol Aging 18(6):609–615

31. Thomas AJ, Perry R, Barber R, Kalaria RN, O'Brien JT (2002) Pathologies and pathological mechanisms for white matter hyperintensities in depression. Ann N Y Acad Sci 977:333–339

32. Tomimoto H, Akiguchi I, Wakita H, Suenaga T, Nakamura S, Kimura J (1997) Regressive changes of astroglia in white matter lesions in cerebrovascular disease and Alzheimer's disease patients. Acta Neuropathol (Berl) 94(2):146–152

33. Tomimoto H, Ihara M, Wakita H, Ohtani R, Lin JX, Akiguchi I, Kinoshita M, Shibasaki H (2003) Chronic cerebral hypoperfusion induces white matter lesions and loss of oligodendroglia with DNA fragmentation in the rat. Acta Neuropathol (Berl) 106(6):527–534

34. Wakita H, Tomimoto H, Akiguchi I, Kimura J (1994) Glial activation and white matter changes in the rat brain induced by chronic cerebral hypoperfusion: an immunohistochemical study. Acta Neuropathol (Berl) 87(5):484–492

35. Wakita H, Tomimoto H, Akiguchi I, Matsuo A, Lin JX, Ihara M, McGeer PL (2002) Axonal damage and demyelination in the white matter after chronic cerebral hypoperfusion in the rat. Brain Res 924(1):63–70

36. Zeman W, Innes JRM (1963) Craigie's Neuroanatomy of the Rat, Academic Press, New York

37. Zhang ZG, Bower L, Zhang RL, Chen S, Windham JP, Chopp M (1999) Three-dimensional measurement of cerebral microvascular plasma perfusion, glial fibrillary acidic protein and microtubule associated protein-2 immunoreactivity after embolic stroke in rats: a double fluorescent labeled laser-scanning confocal microscopic study. Brain Res 844(1–2):55–66